GENERAL EXPERIMENTAL TECHNIQUES

APPLICATION OF CHROMOX FLUORESCENT SCREEN FOR PULSED ELECTRON BEAM DIAGNOSTICS LOW ENERGY

© 2025 V. V. Kurkuchekov*, I. V. Kandaurov, N. Abed, D. A. Nikiforov, D. S. Tanygina

G.I. Budker Institute of Nuclear Physics
Siberian Branch of the Russian Academy of Sciences Russia, Novosibirsk
**e-mail: VVKurkuchekov@inp.nsk.su*

Received April 23, 2024
Revised June 05, 2024
Accepted July 02, 2024

Abstract. The paper reports the results of application of the Chromox alumina ceramic fluorescent screen for measuring the current density distribution in the cross section of an intense low-energy pulsed electron beam. The properties of the screen with gold deposition of different thicknesses were studied: 30 and 300 nm. The 30 nm thick coating has good conductivity and at the same time sufficient transparency (about 5%) for fluorescence emission, which allows visualization of a two-dimensional pattern of the beam current distribution with good spatial resolution. However, such a coating demonstrates limited resistance to the action of a beam with a current of at least 1.5 A (more than 0.6 A/cm2), an energy of 15 keV, and a duration of 1 ms. The 300 nm thick coating has much greater resistance, but is not transparent to fluorescence emission, so the image was recorded "in transmission" of the scintillator plate. This approach allows obtaining an image of the beam imprint, but with a slightly worse spatial resolution.

DOI: 10.31857/S00328162250115e8

1. INTRODUCTION

Electron beams with energy in the range of tens of keV find application in physical materials science as a tool for modeling pulsed thermal loads on material surfaces [1, 2]. Currently, the Budker Institute of Nuclear Physics SB RAS is creating an experimental setup to study the fatigue resistance

of promising materials for the divertor lining and first wall of magnetic confinement fusion reactors under the influence of rapid thermal loads resulting from non-stationary processes in hot plasma. To simulate the thermal shock, it is planned to use a pulsed electron beam with a power density 0.1–1 GW/m ^{2} with a pulse duration of about 1 ms and electron energy of 10–30 keV, operating in a frequency-pulse mode [3]. Information about the distribution of beam power density on the surface of the studied target is fundamentally important in such experiments.

In the existing variety of methods for measuring the distribution of current density (power density) in an electron beam incident on a target, two main groups can be distinguished: a) with local direct measurement of beam parameters; b) based on the registration of radiation resulting from the interaction of beam electrons with the target.

Methods of the first group use a set (matrix) of microcollectors or microcalorimeters performing synchronous point measurements across the beam cross-section [4], or use transverse scanning of the beam with a thin wire or slit diaphragm, behind which a collector is located [5]. The obvious disadvantages of such methods include low spatial resolution and the need for a large number of registration channels, and in the case of scanning diagnostics – a large number of beam pulses required to reconstruct a single profile.

Methods of the second group allow obtaining an image of the beam incident on the target using X-ray [6], transition [7], thermal [8] radiation, as well as luminescence of the target material in the visible range [9]. The type of detected radiation is determined by the beam parameters and technical capabilities of the experiment; however, using a luminescent screen as a target is perhaps the simplest and most easily interpreted method, allowing to obtain a two-dimensional picture of the beam cross-section with good spatial resolution in a single pulse.

For diagnosing a beam with the above-mentioned particle energy, duration, and power density values, the luminescent screen must meet several requirements:

– the emission spectrum of the phosphor should lie in the spectrally sensitive region of CCD and CMOS matrices;

– high light response of the phosphor and its linearity in a wide dynamic range;

– sufficiently short fluorescence decay time and absence of long-term afterglow for measuring the beam profile in consecutive pulses;

– compatibility with high vacuum conditions;

– resistance to heating and thermal shocks;

– mechanical strength and the possibility of manufacturing screens of sufficiently large size at a reasonable cost.

One of the materials that largely meets these requirements is Chromox – alumina ceramic with a 0.5 percent addition of Cr_2O_3 [10]. This type of fluorescent screen is widely known as a beam diagnostic tool in accelerator complexes. Typically, it is used for relativistic (from several MeV to hundreds of GeV) beams of heavy ions or electrons with currents up to 0.1 mA and a total charge arriving at the target during a beam pulse of no more than a few nC [11-14]. Since Chromox ceramic is a good insulator, its use for diagnosing electron beams with energies in the range of several tens of keV and a relatively large total charge per pulse (about 10^{-3} C) faces the problem of charge accumulation on the target, which can significantly distort the recorded beam characteristics.

This paper reports the results of investigating the possibility of using a Chromox screen with metal coating for diagnostics of an electron beam with an energy of 10-20 keV, current up to 2 A, and duration of about 1 ms, designed for studying the resistance of various materials to rapid thermal loads.

2. EXPERIMENTAL SETUP

The scheme for registering the electron beam current distribution is shown in Fig. 1. The beam is generated by a gun with a lanthanum hexaboride thermionic cathode, developed and manufactured at the Budker Institute of Nuclear Physics SB RAS. In the described experiments, the cathode had a ring shape with an outer diameter of 16 mm and an inner diameter of 8 mm. The high-voltage modulator allowed for the formation of beam pulses with currents up to 10 A at an accelerating voltage of up to 20 kV and pulse duration from 20 μs and above with a repetition rate of up to 100 Hz. The beam was formed and transported to the target in an axial divergent magnetic field with a magnitude of 80 mT at the cathode and about 34 mT at the target. A detailed description of the experimental setup, gun design, and power supply systems can be found in [3].

Fig. 1. **a** - Scheme for registering the electron beam current distribution using Chromox fluorescent ceramics. **b** - Vacuum positioner with attached fluorescent screen

The Chromox AF995R fluorescent screen [10] manufactured by Advantech UK Ltd. was attached to a vacuum positioner at a 45° angle to the beam axis at a distance of about 20 cm from the cathode. The screen was a ceramic plate with a thickness of 1 mm and a diameter of 80 mm. This type of phosphor is well-studied and has an extensive history of application in particle beam diagnostics. The ceramic density is 3.85 g/cm^3 with grain sizes of 10-15 μm. The luminescence spectrum consists of lines with wavelengths of 691 nm and 694 nm with fluorescence decay times of 3.4 ms and 6.7 ms, respectively. Chromox ceramics is compatible with high vacuum, withstands thermal loads well, has a high photon yield ($5 \cdot 10^4$ photons/MeV), and linear response.

The screen luminescence was recorded by a CCD camera SDU-285 [15]. The camera is equipped with a SONY ICX285AL matrix with a resolution of 1392×1040 pixels with a size of $6.45 \times 6.45\ \mu m^2$. The exposure time in the experiments was 5 ms.

3. EXPERIMENTAL RESULTS

Figure 2 shows images of the Chromox screen glow with a clean surface at different magnitudes of the guiding magnetic field. The beam had a current of about 1 A with an accelerating voltage of 10 kV and a pulse duration of 1 ms. The images show strong distortion of the ring shape of the beam and its spreading due to charge accumulation on the target. At relatively low accelerating voltages (less than 10 kV), even blocking of the gun emission current was observed on the current oscillograms.

Fig. 2. Images of the Chromox screen glow under the influence of an electron beam at different magnitudes of the guiding magnetic field

3.1. Chromox screen with gold coating of 30 nm thickness

To eliminate effects associated with charge accumulation on the surface, a metal mesh tightly adjacent to the fluorescent screen can be used, or one sputtered on its surface. However, the image of the mesh will inevitably overlap with the beam image and degrade the quality of the obtained data [16]. This can be avoided by applying a thin metal film to the phosphor, which will ensure good conductivity of the surface while having sufficient transparency for phosphor radiation. The coating film should be uniform and resistant to chemical interaction with the screen material.

Gold was chosen as the material for this coating because this metal has good conductivity and is one of the most chemically inert. The coating thickness was selected based on the dependence of the specific conductivity of the gold film on its thickness. Thus, at a thickness of about 20 nm, the specific conductivity of the coating reaches a maximum and then practically does not change [17]. In our work, the coating thickness was about 30 nm. For such a gold film, the light transmission at a wavelength of 693-695 nm is about 5% [18], which provides sufficient brightness for image registration. Gold deposition was carried out by thermal vacuum method, and the film thickness was measured using a silicon witness wafer placed next to the screen being coated. Note that with a deposition thickness of about 30 nm and the ceramics grain size of 10-15 μm stated by the manufacturer, it is difficult to judge the continuity of the metal coating on the surface. To control conductivity, the resistance of the deposited film was measured with a Fluke15B+ multimeter. The

resistance value between the grounded screen holder and any point on the coating did not exceed 30 Ohms.

An image of the beam glow on the screen with a 30 nm gold coating is shown in Fig. 3. The emission current here was 1 A with an accelerating voltage of 12 kV and a pulse duration of 0.4 ms. Unlike experiments with uncoated ceramics, the beam imprint has the shape of a clear ring without distortions. The outer diameter of the imprint is 24 mm, which corresponds to the calculated beam expansion in the diverging guiding magnetic field. As can be seen, along with the beam imprint, there is a non-uniform background in the image. This background is due to both the illumination of the screen by radiation from the hot cathode and the presence of scattered electrons arising from the reflection of part of the beam electrons from the screen material. As is known from numerous literature sources (see, for example [19]), for an incidence angle of 45°, the current reflection coefficient of electrons with an energy of about 10 keV from an aluminum target is 15-20%. In the presence of a guiding magnetic field, the reflected electrons return to the gun, where some of them are reflected back by the cathode potential, and the rest are partially reflected by the external elements of the gun structure (stainless steel), and eventually these twice-reflected electrons return to the target again.

Fig. 3. Image of the beam print on the Chromox screen with 30 nm gold coating

For direct comparison of the beam print brightness with the current density value corresponding to the respective image area, the dependence of the phosphor's light response on the number of particles must be linear. A detailed study of various luminescent screens conducted at GSI (Helmholtz Centre for Heavy Ion Research, Darmstadt, Germany) [20] shows that the Chromox fluorescent screen has good response linearity. However, this characteristic was measured on ion beams with energy of 295 MeV/a.m.u. without metallic coating on the surface.

The fundamental differences in beam parameters and the presence of a metallic screen coating make it necessary to verify the linearity of the light response in the presented experiments. For this purpose, the gold-coated screen was irradiated with an electron beam at various particle energies, currents, and pulse durations. The camera settings remained unchanged throughout the experimental series. The obtained results are shown in Fig. 4. The x-axis represents the number of electrons in the beam per pulse. The y-axis shows the integrated brightness of the beam print. The integration was performed over a rectangular area occupied by the beam print. The size and position of the integration area were constant during the processing of all images. The experimental dependencies obtained at different accelerating voltages are plotted on the graph. The dashed lines show linear functions fitted to the corresponding dependencies using the least squares method. The non-zero brightness values at

zero current are due to screen illumination by radiation from the gun's hot cathode (the corresponding level is shown on the graph with a red cross) and the presence of background from scattered electrons. Nevertheless, the light response depends linearly on the number of beam electrons.

Fig. 4. Dependence of the integral brightness of beam imprints on the number of beam electrons

It should be noted that in a series of experiments to check the linearity of the light response, the fluorescent screen was subjected to a total exposure of about 500 beam pulses, in which the current did not exceed 0.9 A with electron energy of 15 keV and pulse duration up to 1 ms. Rare cases of breakdowns were observed on the screen surface, but no deterioration in image quality was observed at the end of the series. When the beam current was increased to 1.5 A and above, the frequency and brightness of surface discharges increased significantly (see Fig. 5a). The traces of discharges were irreversible: once they appeared, they remained visible in subsequent images as bright broken lines. As these traces accumulated, the image quality noticeably deteriorated; an example of such an image is shown in Fig. 5b. The degradation of the imprint quality was accompanied by the appearance of strong noise on the beam current oscillograms and partial blocking of the emission current, as was observed in the case of ceramics without metal coating. In total, in this series of experiments, the screen was exposed to about 50 beam pulses with a current of 1.4-2 A, with an accelerating voltage of 13-15 kV and a duration of up to 1 ms. After extracting the screen from the vacuum chamber, control measurements of the gold coating resistance showed its increase by a factor of 10^4-10^5 times, with the conductivity deteriorating most significantly at the periphery of the coating in areas not directly exposed to the beam.

Fig. 5. **a** - Example of an image of a discharge occurring on the surface of a fluorescent screen. **b** - Image of a beam imprint and multiple traces from discharges after several dozen pulses.

3.2. Chromox screen with 300 nm gold coating

The instability of the 30 nm coating led to the decision to increase the durability of the coating by increasing its thickness. The previously applied coating was ground off with an abrasive, and then a layer of gold about 300 nm thick was deposited. Such a coating is largely transparent both to beam electrons and to accompanying bremsstrahlung radiation. For example, in the continuous slowing down approximation, the range of 15 keV electrons until complete stoppage in gold is approximately 750 nm [21], and the transmission coefficient for photons with an energy of 5 keV exceeds 0.6 [22]. Although the gold coating of this thickness is not transparent to the fluorescence spectrum, the good transparency of Chromox ceramics for its own radiation at a wavelength of 693 nm (attenuation coefficient is 8 cm^{-1} [10]) allows detecting fluorescence "in transmission" through the screen plate.

The appearance of the screen with coating and the registration scheme are shown in Fig. 6. The resistance of the coating did not exceed approximately 0.6 Ohm between any two points on the surface.

Fig. 6. a – The appearance of the Chromox fluorescent screen with a 300 nm thick gold coating. **b** – Scheme for registering the beam current distribution by radiation passing through the scintillator plate.

Fig. 7 shows an example of a beam imprint image obtained in such an experimental configuration. As can be seen, the contrast of the obtained images has significantly improved, which is associated with the disappearance of parasitic illumination from the hot cathode of the electron gun, as well as greater transparency of the 1 mm thick Chromox plate for its own radiation compared to the gold coating with a thickness of about 30 nm (transmission coefficients are 45% and about 5%, respectively). At the same time, the finite thickness of the ceramic plate leads to some blurring of the image and, consequently, a decrease in the spatial resolution of diagnostics.

Fig. 7. Image of the beam imprint luminescence on the back side of the Chromox fluorescent screen with a 300 nm thick gold coating

The screen was removed from the vacuum chamber after approximately 100 beam pulses with an energy of 15 keV, a current of 1.6 A, and a duration of 1 ms. Control resistance measurements showed that the coating resistance did not change compared to the original one before beam irradiation.

4. CONCLUSION

1. It has been shown that a fluorescent screen made of Chromox alumina ceramics with metallic coating can be successfully used for diagnostics of current density distribution in the cross-section of a pulsed electron beam with energy of 10-20 keV, current density at the target of 1 A/cm ^{2} and duration of about 1 ms. Chromox ceramics is resistant to thermal shocks produced by the beam.

2. Gold coating with thickness of about 30 nm, deposited by thermal vacuum method, has sufficient transparency (about 5%) to ceramic fluorescent radiation and allows obtaining images with high spatial resolution, however has limited resistance to beam exposure. The coating loses its conductive properties after several dozen beam pulses with energy of about 15 keV, current over 1.5 A (current density at the target about 1 A/cm ^{2}) and duration of 1 ms.

3. A measurement scheme with gold coating of about 300 nm and "transmission" image registration of the fluorescent screen was considered. Coating of such thickness proved to be significantly more resistant to beam exposure and did not reduce its conductive qualities after approximately 100 beam pulses with energy of 15 keV, current of 1.6 A and duration of 1 ms. This

measurement scheme provides greater brightness and image contrast and is free from parasitic illumination from the gun cathode, but light scattering in the screen material leads to some decrease in spatial resolution of diagnostics.

ACKNOWLEDGMENTS

The authors thank A.V. Petrenko for providing Chromox ceramics. The authors are grateful to D.I. Skovorodin and Yu.A. Trunev for useful discussions.

FUNDING

This work was supported by the Russian Science Foundation (grant 22-72-00037).

CONFLICT OF INTERESTS

The authors declare that they have no conflict of interest.

REFERENCES

1. *Loewenhoff T., HiraiT., Keusemann S. et al.* // J. Nucl. Mater. 2011. V. 415. № 1. P. S51. http://doi.org/10.1016/j.jnucmat.2010.08.065
2. *Vyacheslavov L., Arakcheev A., Burdakov A. et al*. // AIP Conf. Proc. 2016. V. 1771. № 1. P. 060004. https://doi.org/10.1063/1.4964212
3. *Kurkuchekov V.V., Abed N., Ivanov A.V., Kandaurov I.V., Nikiforov D.A.* // VANT. Ser. Thermonuclear Fusion. 2024. V. 47. No. 2.
4. *Schuch R.L., Kelly J.G.* // Rev. Sci. Instrum. 1972. V. 43. No. 8. P. 1097. https://doi.org/10.1063/1.1685854
5. *Forck P.* arXiv preprint arXiv:2009.10411. 2020. https://doi.org/10.48550/arXiv.2009.10411
6. *Kurkuchekov V., Kandaurov I., Trunev Y.* // J. Instrum. 2018. V. 13. No. 5. P. P05003. http://doi.org/10.1088/1748-0221/13/05/P05003
7. *Silva T.F., Bonini A.L., Lima R.R. et al.* // Rev. Sci. Instrum. 2012. V. 83. No. 9. https://doi.org/10.1063/1.4748519
8. *Astrelin V.T., Burdakov A.V., Zabolotsky A.Yu. et al.* // PTE. 2004. No. 2. P. 66. https://doi.org/10.1023/B:INET.0000025201.89969.ae
9. *Ischebeck R., Prat E., Thominet V., Loch C.O.* // Phys. Rev. ST Accel. Beams. 2015. V. 18. No. 8. P. 082802. http://dx.doi.org/10.1103/PhysRevSTAB.18.082802

10. *McCarthy K.J., Baciero A., Zurro B. et al.* // J. Appl. Phys. 2002. V. 92. No. 11. P. 6541. https://doi.org/10.1063/1.1518133
11. *Bal C., Bravin E., Lefèvre T. et al.* // Proceedings of DIPAC 2005. Lyon, France. 2005. P. 57. No. CERN-AB-2005-067.
12. *Forck P., Andre C., Becker F. et al.* // Proceedings of DIPAC2011, Hamburg, Germany, MOPD53. P. 170.
13. *Good J., Kube G., Leuschner N. et al.* // J. Phys. Conf. Ser. 2013. V. 425. No. 12. P. 122012. http://dx.doi.org/10.1088/1742-6596/425/12/122012
14. *Lumpkin A.H., Yang B.X., Berg W.J. et al.* // Nucl. Instrum. Methods. Phys. Res. A. 1999. V. 429. No. 1-3. P. 336. https://doi.org/10.1016/S0168-9002(99)00075-3
15. Camera description http://www.sptt.ru/sptt/catalog.php?l
16. *Berg W., Ko K.* // AIP Conf. Proc. 1992. V. 281. No. 1. P. 279. https://doi.org/10.1063/1.44348
17. *Antonets I.V., Kotov L.N., Nekipelov S.V., Karpushov E.N.* // JTF. 2004. V. 74. No. 11. P. 102.
18. *Axelevitch A., Gorenstein B., Golan G.* // Physics Procedia. 2012. V. 32. P. 1. http://dx.doi.org/10.1016/j.phpro.2012.03.510
19. *Goldstein J., Newbury D., Michael J. et al.* Scanning electron microscopy and X-ray microanalysis. New York: Springer, 2018. http://dx.doi.org/10.1007/978-1-4939-6676-9
20. *Renuka K., Ensinger W., Andre C., Beeker F., Forck P., Haseitl R., Reiter A., Walasek-Hohne B* . // BIW2012 Proceedings. Newport, VA, USA. TUPG022. 2012. P. 183.
21. *Berger M.J.* ESTAR, PSTAR, and ASTAR: Computer programs for calculating stopping-power and range tables for electrons, protons, and helium ions. NIST. US Department of Commerce. 1992.
22. *Hubbell J.H., Seltzer S.M.* X-Ray Mass Attenuation Coefficients. NIST, US Department of Commerce, 1995. https://dx.doi.org/10.18434/T4D01F

FIGURE CAPTIONS

Рис. 1. **a** - Scheme for recording electron beam current distribution using Chromox fluorescent ceramics. **b** - Vacuum manipulator with attached fluorescent screen.

Рис. 2. Images of Chromox screen luminescence under electron beam exposure at different guiding magnetic field values.

Рис. 3. Image of beam footprint on Chromox screen with 30 nm gold coating.

Рис. 4. Dependence of integral brightness of beam footprints on the number of beam electrons.

Рис. 5. **a** - Example image of discharge occurring on fluorescent screen surface. **b** - Image of beam footprint and multiple discharge traces after several dozen pulses.

Рис. 6. **a** - External view of Chromox fluorescent screen with 300 nm gold coating. **b** - Scheme for recording beam current distribution by radiation passing through the scintillator plate.

Рис. 7. Image of beam footprint luminescence on the reverse side of Chromox fluorescent screen with 300 nm gold coating.

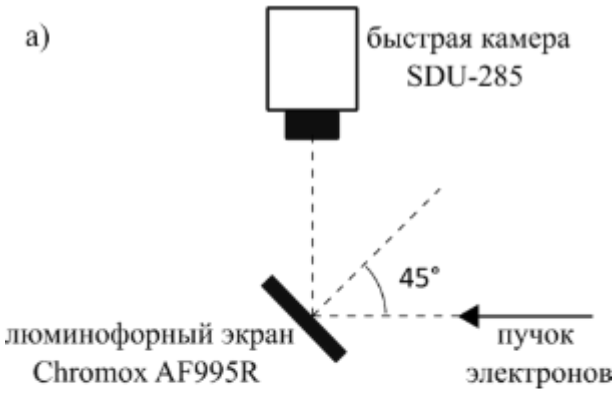
а)
быстрая камера
SDU-285
45°
люминофорный экран
Chromox AF995R
пучок
электронов
б)

Fig. 1.

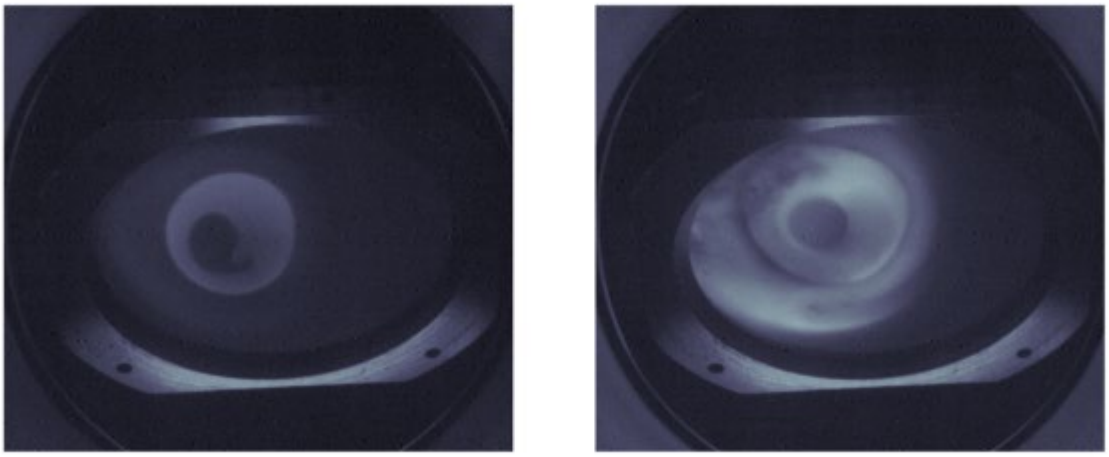

Fig. 2.

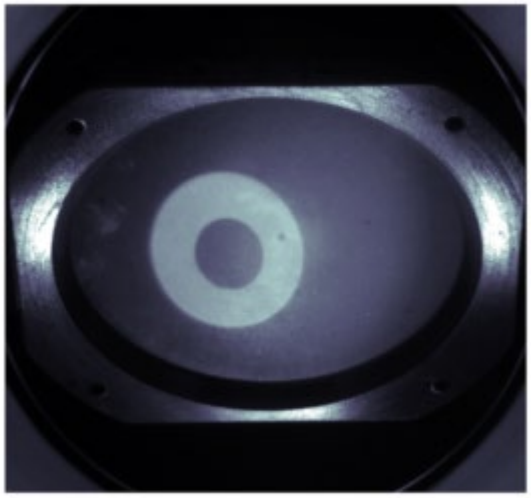

Fig. 3.

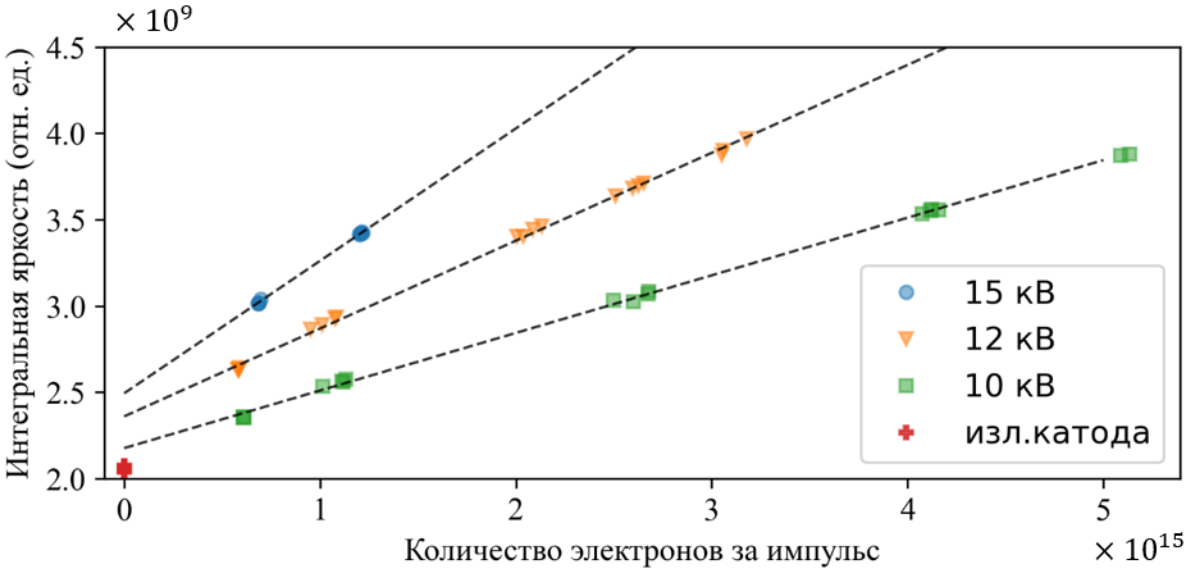
× 10^9
4.5
4.0
3.5
3.0
2.5
2.0
Интегральная яркость (отн. ед.)
0
1
2
3
4
5
× 10^15
Количество электронов за импульс
15 кВ
12 кВ
10 кВ
изл.катода

Fig. 4.

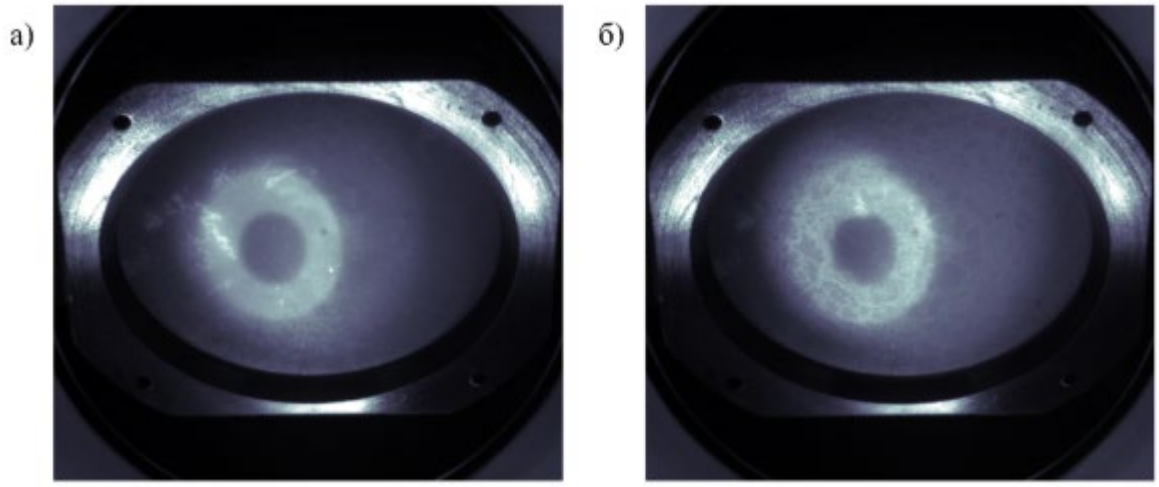
а)
б)

Fig. 5.


а)
б)
быстрая камера
SDU-285
люминофорный экран
Chromox AF995R
45°
пучок
электронов

Fig. 6.

Fig. 7.